Proceedings of International Conference on Heat Exchanger Fouling and Cleaning - 2013 (Peer-reviewed)
June 09 - 14, 2013, Budapest, Hungary
Editors: M.R. Malayeri, H. Müller-Steinhagen and A.P. Watkinson
Published online
www.heatexchanger-fouling.com

EFFECT OF FOULING ON THE THERMAL PERFORMANCE OF CONDENSERS AND ON THE WATER CONSUMPTION IN COOLING TOWER SYSTEMS

X. Wu[1*], and L. Cremaschi[1]

[1] Oklahoma State University, School of Mechanical and Aerospace Engineering, Stillwater, OK, USA
xiaoxiao.wu@okstate.edu, cremasc@okstate.edu
*Corresponding Author

ABSTRACT

Circulating water in cooling tower systems contains an excess amount of mineral ions. When this hard water is heated inside condensers, these minerals precipitate and the deposition of unwanted material on the heat transfer surface reduces the overall heat transfer performance. Fresh water is often used to mitigate fouling but then water conservation might become a concern.

This paper focuses on fouling effects on the thermal and hydraulic performance of condensers and on the water consumption of cooling tower systems. Two braze plate heat exchangers and a smooth tube-in-tube heat exchanger was experimentally investigated under fouling operating conditions. A model for the mineral species dissociation and mineral precipitation on the heat transfer surfaces was developed. By considering a semi-empirical relation for the fouling deposition strength factor, the simulation results predicted the fouling thermal resistance with an error of 30%. Model limitations and research needs for potential improvements are discussed.

INTRODUCTION

In water cooled condensers, heat is rejected to the water circulating in cooling tower loops. Since large amount of inversely-soluble minerals, such as calcium carbonate and magnesium carbonate, are often contained in the water, the evaporation process in the cooling tower increases the mineral concentration. When the reclaimed water is heated up in the condensers, the solubility of the minerals decrease and precipitation occurs (Cho *et al.*, 2003). Aside from precipitation, other fouling mechanisms are particulate fouling, biological fouling and corrosion fouling (Haider *et al.*, 1991). Since cooling tower water is often pre-treated with biological and corrosion inhibitors, the last two types of fouling mechanism can be more or less controlled (Walker, 1976). Previous researcher pointed out that fouling formation is a combination of deposition and removal processes (Kern & Seaton, 1959) and an illustration of which is shown in Fig. 1.

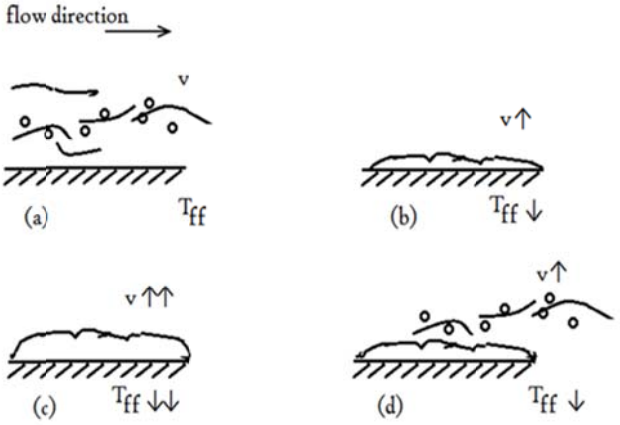

Fig. 1 Illustration of precipitation fouling and particulate fouling on a simple flat plate

Fluid with fouling agent flows across the heated surface with velocity v and fluid film temperature near the wall surface, T_{ff}, as indicated in Fig. 1(a). Fluid is heated up and an increase of fluid temperature leads to a drop of local solubility, thus previously dissolved calcium carbonate in the fluid begins to precipitate and a layer of fouling deposit begins to form on the heat transfer surface, shown in Fig. 1 (b). The layer of fouling increases the thermal resistance between the heated surface and fluid, leading to the reduction of film temperature on the top of the surface. Since the solubility of calcium carbonate increases with decreasing temperature (Flynn & Nalco, 2009), then the fouling precipitation rate decreases due to lower T_{ff}, see Fig. 1(c). Meanwhile, due to the flow barrier caused by the fouling deposit, the local fluid velocity and shear stress increase accordingly. A removal process of clusters of fouling deposit might occur if the shear stress is high enough to carry particles away from the fouling layer, as illustrated in Fig. 1(d). The removal of fouling reduces the thermal resistance, thus the fouling precipitation restarts due to higher local water fluid film temperature, T_{ff} near the plate. The local water fluid film temperature and mineral concentration drive the precipitation process. The thickness of fouling inside the condensers is expected to reach a

limiting threshold in which the process of fouling deposition and fouling removal are in equilibrium. If the particles do not obstacle the flow, precipitation and removal process would recur, and Fig. 1(c) and (d) show this situation, and the thermal resistance offered by the mineral deposition layer on the heat transfer surface approaches an asymptotic value, referred to as the asymptotic fouling resistance.

LITERATURE REVIEW

One of main driving forces of fouling in heat exchangers is the mineral concentration, especially calcium concentration. Langelier proposed an index to evaluate the solubility of $CaCO_3$ in nature water, which is known as Langelier Saturation Index or LSI (Langelier, 1936). Mathematically, LSI is expressed as the algebraic difference between actual pH of a water sample and its computed saturation pH, which is the pH at which the calcium concentration in given water sample is in equilibrium with the total alkalinity. Eq. (1) is used to calculate the LSI and Eq. (2) is one method to estimate the saturation pH of water.

$$\mathrm{LSI} = pH_{actual} - pH_{sat} \tag{1}$$

$$pH_{sat} = 12.18 + 0.1 \log_{10}(TDS) - 0.0084\,(T_w) - \log_{10}(Ca) - \log_{10}(M_{alkalinity}) \tag{2}$$

If the index equals zero, the water is in equilibrium state; a plus sign of the index means a tendency of precipitation and a minus sign indicating a tendency of dissolving. Cremaschi *et al*. (2011) adopted the definition of "water fouling potential" to describe the scaling conditions of the water.

The evaluation of water fouling potential was based on LSI and other minerals, as shown in Table 1. LSI lower than 1 was defined as low fouling potential water, where slight and low scaling formation were expected. LSI between 1 and 2 were for medium fouling potential water and moderate scaling formations were expected. Any LSI higher than 2 was grouped in the high fouling potential water category, which represents very aggressive water in terms of mineral precipitation.

Several researchers worked on evaluating other parameters that influence fouling in heat exchangers. Karabelas *et al*. (1997) conducted experiments to reveal that internal geometry of BPHEs (brazed plate heat exchangers) would impact the fouling resistance, plates with corrugation angle of 30° had more tendencies to foul than ones with corrugation angle of 60°. Similar observation was reported by (Grandgeorge *et al.*, 1998), (Cremaschi, *et al.*, 2011) and (Thonon *et al.*, 1999). Thonon *et al*. (1999) also investigated in the fouling potential of different types of particles and they claimed that fouling rate of TiO_2 was much lower than $CaCO_3$. Experiments regarding to the impacts of internal geometry on fouling formation in tubular heat exchangers was conducted by Webb & Li (2000), in their work, the fouling mechanism is a combination of precipitation and particulate fouling, and they observed that more minerals would precipitate in enhanced tubes than smooth tubes, indicating that the asymptotic fouling resistance has a strong dependence on internal geometry of the tubular heat exchangers.

Numerical analysis was also developed to describe fouling characteristics on heat transfer surface. Hasson *et al*. (1978) developed a deposition rate model to predict $CaCO_3$ fouling rate in acid and alkaline solution. Chamra & Webb (1994) proposed a semi-theoretical model to predict the asymptotic fouling resistance in enhanced tubes, which considered solution concentration, velocity and particle size. Grandgeorge *et al*. (1998) studied the impacts of flow velocity on fouling formation in corrugated BPHEs and a fouling rate global model was proposed to predict the asymptotic deposit on the heat transfer surface.

EXPERIMENTAL METHODOLOGY

High and medium water fouling potentials were developed in our laboratory to replicate the fouling mechanism of brazed-plate type condensers in cooling tower applications. The experimental apparatus mainly consisted of two loops: a water loop and a refrigerant loop, sharing the same test condenser. In the water loop, water was progressively concentrated and controlled in saturated conditions while running through the test condenser, which was installed in series with a small cooling tower, serving primarily as a mineral concentrator.

Table 1 Typical water chemistry for different water quality (adapted from(Cremaschi, *et al.*, 2011))

Fouling Potential	Total Hardness	Calcium (as $CaCO_3$)	Magnesium (as $CaCO_3$)	M-Alkalinity (as $CaCO_3$)	P-Alkalinity (as $CaCO_3$)	Chloride (ppm)	Sulfate (ppm)
Low	180-358	13-92	16-53	54-91	4-15	102-258	64-133
Medium	345-533	18-265	28-109	106-289	6-77	208-884	139-603
High	557-1765	129-391	76-183	204-1813	58-417	491-1947	319-1947
Fouling Potential	**Sodium (ppm)**	**Iron (ppm)**	**Copper* (ppm)**	**pH**	**Total Dissolved Solid (ppm)**	**EC (μS/cm)**	**LSI (-)**
Low	43-93	<0.1	NA	8.2-8.4	428-897	649-1359	< 1.0
Medium	87-373	<0.1	NA	8.4-8.8	826-2896	1251-4360	1.1 – 2
High	192-741	<0.1	NA	9.0-9.6	2000-7971	3030-11690	2.1 – 3.8

*water was circulated in copper pipe of about 22 feet (6.7 m) of length and 1 inch (2.54 cm) nominal pipe size diameter. Copper particles were observed in the water since a change of water color was observed after about 1-2 weeks of continuous run

During operation, water became supersaturated inside the condenser, where it was rapidly heated up by the saturated refrigerant and mineral precipitation occurred due to a drop of local solubility. There were not any filters used in the water loop and more details of the experimental methodology and data reduction used in the present work were given in authors' previous work (Cremaschi *et al.*, 2012; Cremaschi, *et al.*, 2011). From authors' previous work, brazed plate heat exchangers (BPHEs) with different geometries were tested at different water scaling conditions. In order to provide some comparison of the fouling characteristics between BPHEs and tube-in-tube heat exchangers (TTHEs), a smooth tubular heat exchanger with the same heat transfer area as the BPHEs was also tested and the results are given in (Wu & Cremaschi, 2012). In the present paper, data of energy performance of the condensers and water use in the cooling tower in fouling conditions are presented. The experimental data also served to verify a general first principle model for the heat and mass balances during fouling operating conditions of condensers. The model considers water minerals content, water temperature, flow velocity, and geometry of the heat exchangers as input parameters and the model can predict the fouling resistance with time within 30% accuracy, however it generally under-predicted the fouling thermal resistance at the beginning stage of fouling formation and in the case of severe particulate fouling.

DISCUSSION OF THE EXPERIMENTAL DATA

A. Impacts of fouling on energy performance of condensers

From the data presented in the current work and the authors' previous work, the overall heat transfer coefficients and UAs for BPHEs and the TTHEs decreased with time due to fouling (Cremaschi, *et al.*, 2012; Cremaschi, *et al.*, 2011; Wu & Cremaschi, 2012). The LMDT method was used in data reduction analysis of the present work and only the saturation region was used as reference parameter for the refrigerant operating conditions. At the very beginning of fouling tests, the test exchangers were new and we consider the thermal and hydraulic performance as "clean conditions". As indicated in Eq.(3), the total thermal resistance for heat exchanger under clean conditions $R_{tot,clean}$ includes thermal resistance due to convection heat transfer on the refrigerant side (R_{ref}), conduction through the tube wall or plate thickness (R_k), and convection heat transfer on the water side (R_w). Once fouling appears, the thermal resistance increases; after several months of operation, a measurable fouling resistance (R_f) is added to the previous terms, as shown in Eq. (4).

$$R_{tot,clean}=R_{ref}+R_k+R_w \quad (3)$$

$$R_{tot,fouled}=R_{ref}+(R_k+R_f)+R_w \quad (4)$$

By solving the system of two equations (3) and (4) in two unknowns (R_w for both clean and fouled conditions) Table 2 was calculated and it gives the thermal resistance for the BPHEs and TTHE tested in the present work. The total thermal resistance of each heat exchanger was considered as the sum of four terms in the right hand side of Eq.(4). Each term was normalized with respect to the convective thermal resistance of water (R_w) in clean condition, which was estimated from the measured flow rates and temperatures based on the classic convective equation in (Incropera *et al.*, 2006) for TTHE and the correlation in (Ayub, 2003) for BPHEs. The conduction thermal resistance (R_k) was estimated from the materials and geometry of the tested heat exchangers. The total thermal resistance in clean and fouled conditions was directly measured from the heat transfer experiments of the present work. The convective thermal resistance of refrigerant side (R_{ref}) was calculated from the difference between total thermal resistance and water-side thermal resistance (including conduction resistance) in clean operating conditions. Since the refrigerant operating conditions were purposely set constant during the fouling period, we assumed that the refrigerant side thermal resistance was unaffected by the water-side fouling, that is, the heat transfer areas of superheat vapor, saturated two phase, and sub-cooled liquid refrigerant did not vary between clean and fouled operating conditions. It should be noted that, for slight fouling conditions, this assumption is reasonable; however, in severe fouling conditions, we expect some variations on the refrigerant side convective thermal resistance due to the decrease of heat flux at the refrigerant-wall interface.

Table 2 Thermal resistance increase inside heat exchangers due to fouling formation

Heat Exchangers	Condition	Rk [-]	Rref [-]	Rw [-]	Rf [-]	Rtot [-]
BPHE A1 (φ=30°)	Clean	0.08	0.78	1	0	1.86
	Fouled	0.08	0.78	1.1	3.19	5.15
BPHE A2 (φ=63°)	Clean	0.13	0.8	1	0	1.93
	Fouled	0.13	0.8	1.06	0.7	2.69
Smooth tube	Clean	0.09	0.46	1	0	1.55
	Fouled	0.09	0.46	1.2	0.42	2.17

Table 2 indicates that the dominant thermal resistance is always the water side. This result was expected since the convective heat transfer coefficient for two-phase refrigerant is usually higher than that of water in single phase flow. At the end of the fouling tests, the fouling thermal resistance of smooth tube was 42% of the water thermal resistance in clean condition and 70% for BPHE A2 with corrugation angle of 63°. For BPHE A1 with corrugation angle of 30°, the additional thermal resistance due to fouling was 3.19 times of the water thermal resistance in clean condition. This was an extreme case for which the BPHE was partially blocked by particulate fouling.

The increase of thermal resistance due to fouling formation varies according to the type of heat exchanger, test condition and water quality. Table 2 indicates experiments conducted on heat exchangers functioning as refrigerant to water condensers with high fouling potential water. The total thermal resistance increased by 2.77 times for A1 plate and 40% both for A2 plate and smooth tube-in-tube heat exchanger. Due to fouling formation, the water side free flow area of the heat exchanger decreased, yielding to augmentation of the local water flow velocity. However,

the minerals might deposit on the bottom of channels formed by the corrugations of two adjacent plates and hindered the enhancement configuration, thus the water side convective thermal resistance (R_w) increased. As shown in the last column of Table 2, the overall effect of fouling is an increase of thermal resistance of the heat exchangers.

Fig. 2 shows the water temperature difference between inlet and outlet of the two BPHEs (A1&A2) and a TTHE condenser. All of them were tested with same refrigerant saturation temperature, degree of de-superheat and same water fouling potential. This resulted in approximately same heat flux in initial clean conditions and then the refrigerant and water flow rates were set constant throughout the test periods. TTHE data was from the current work and BPHEs data were adapted from authors' previous work (Cremaschi, *et al.*, 2012). Since the water flow rate was controlled to be constant for all the tests, the decrease of water temperature difference across the condenser has similar trend as the heat flux. The A1 plate with corrugation angle of 30°, shown as diamond points, had a sharp temperature drop of 0.6°C due to fouling formation; the heat flux for which in clean conditions were about 11kW/m^2, and after 30 days of fouling tests, the heat flux decreased by 28%. The A2 plate with corrugation angle of 63° experienced a small temperature decrease of 0.2°C and the heat flux degradation was within 5% in 55 days with respect to clean conditions. The trend of TTHE was quite similar as A2 plate, in 60 days of operation, a decrease of 8% in heat flux was observed and by the end of the fouling test water temperature difference decreased by 0.4°C.

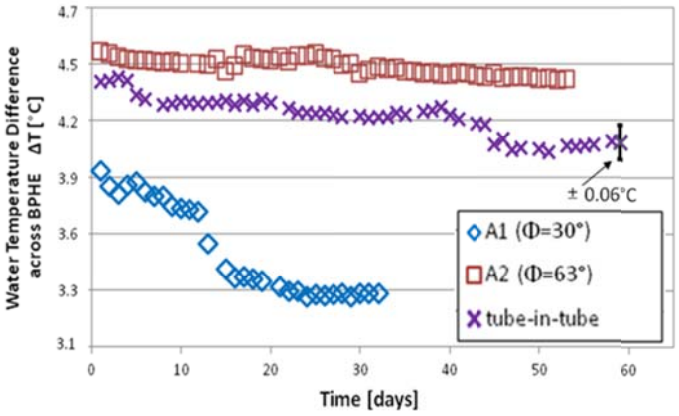

Fig. 2 Water temperature difference across tested heat exchangers in fouling tests

The hydraulic performance of the heat exchangers is presented in the form of pressure drop penalty factors (PDPF) in Fig. 3. TTHE data was from the current work and BPHEs data were adapted from authors' previous work (Cremaschi, *et al.*, 2012). Pressure drop across the condensers in clean conditions are given in the legend. PDPF values for each test were calculated according to Eq. (5) and they represented the ratio of water side pressure drops measured in fouled conditions and the corresponding ones measured in clean conditions. For instance, A2 plate had a PDPF of 1.1 after 55 days of fouling tests, which means a 10% of increase of pressure drop in fouled condition was observed by the end of the test with respect to clean conditions. A1 plate experienced a localized blockage of the mini-channels and as a result, the pressure drop increase by 30%.

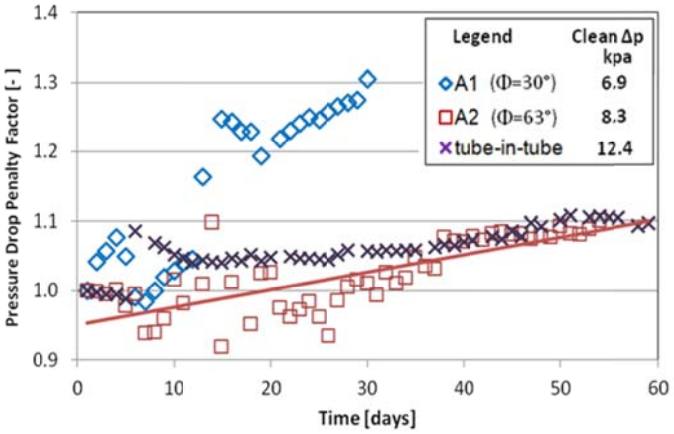

Fig. 3 Pressure drop penalty factor across tested heat exchangers in fouling tests

$$PDPF=\Delta P_{w,f}/\Delta P_{w,c} \quad (5)$$

The cross points in Fig. 3 indicate the pressure drop across the TTHE; since it had large free flow cross sectional area than the braze plate-type heat exchangers, it was not subjected to severe clogging due to fouling. As shown in Fig. 3, at about day 5, the tube PDPF increased suddenly. This phenomenon is generally due to localized flow blockage from particulate fouling, in which particles attached on the surface and created a significant resistance to the water stream. After day 5, the increase of the PDPF for the TTHE was minor and the pressure loss was about 10% higher than the initial pressure drop in clean conditions.

B. Water losses in cooling tower due to fouling

Fouling formation inside the heat exchangers is strongly dependent on the water quality in cooling tower systems, which is related to the water consumption since fresh make-up water is usually added to dilute the recycled water coming from the cooling tower. This mixing reduces the fouling potential of the water circulating through the condenser.

Fouling tests were conducted on BPHEs with two corrugation angles and a smooth TTHE that operated as refrigerant condensers. The system was a small scale 3 ton cooling tower system operating in controlled environmental conditions in laboratory. All the fouling tests were conducted with medium and high fouling potential water. Water with low fouling potential was used in the initial stage of the tests and charged to the system as make-up water. Because of the water evaporation in the cooling tower, water in the system reached medium and high water fouling potentials in 1 to 2 weeks. For the case of high fouling potential (high FP) water, the water loss due to evaporation at the cooling tower was about 88% of the entire water (the total amount of fresh make-up water and reclaimed water) consumed in the cooling tower system at the end of two month period. The actual water losses in the system ranged from 84% to 93% depending on the geometry and refrigerant saturation temperature in the condensers. For the case of medium fouling potential (med

FP) water, the water losses were about 83% of the entire water consumed in the cooling tower system and this value was practically independent from the fouling formation. This can be explained with the fact that, in medium fouling potential water application, the impact of fouling thermal resistance on the water-side cooling capacity was not as significant as for the case of high fouling potential water. In our tests, about 100 gallon of water were initially charged in the cooling tower system and the evaporation rate was about 10 gal/day for medium fouling potential case and 15gal/day for the case of high fouling potential water. Due to evaporation in the cooling tower loop, minerals contained in recycled water become concentrated and reached the solubility limits. For the fouling test on a smooth TTHE condenser at high fouling potential water, due to water evaporation in the cooling tower, the amount of Ca^{2+} in the water loop practically increased linearly with time. In two weeks without any water treatment, the Ca^{2+} concentration doubled, and the water losses exceed 50% of the total water consumption in the system. After two months of continuous operation, water losses due to evaporation reached about 85% of the total water consumption and the Ca^{2+} concentration increased by more than 6 times. A dilution of the recycled water with more fresh water might have relieved the fouling issues but it would have increase the fresh water usage. Cycle of concentration provides a measure of the accumulation of dissolved minerals in the circulating cooling water. It is defined in Eq. (6) (Beychok, 1952) and it is practically the ratio of concentration of chlorides in the circulating water and in the make-up water. High cycles of concentration mean high fraction of recycled water from the cooling tower in the main stream that flows in the condenser.

$$cycle = \frac{[Cl^-]_{circulate}}{[Cl^-]_{makeup}} \tag{6}$$

In the present fouling experiments on BPHEs and on TTHE, in the case of condensation saturation temperature of 40.5°C, the concentration cycles ranged from 4 to 7.3. An increase of condensation temperature from 40.5°C to 49°C augmented the cycles of concentration to 14~16.1 because the evaporation rate in the cooling tower was higher when the water temperature entering the cooling tower increased.

In actual cooling tower loops, water treatment plants and filter systems help mitigating the mineral precipitation and particulate fouling and the time required to achieve medium or high fouling potential water is usually longer than two months. It was reported that cooling tower could operate at 5 cycles of concentration if fouling inhibitors are used (Betz, 1991). Cycles greater than 5 are sometimes used in regions of short supply of water. If the cycles of concentration increase then less fresh or domestic water is used but the water fouling potential of the cooling water in the system increases. This yields to higher propensity to mineral precipitation on the heat transfer surfaces where the solubility limits are reached. In order to balance the water consumption and fouling formation in the cooling tower systems, Cho *et al*., (2006) examined the effect of electronic antifouling technology with a solenoid coil on fouling mitigation in cooling tower systems at high cycles of concentration and they reported that the physical water treatment was able to reduce the fouling resistance by 70% at 5 cycles and by 60% at 10 cycles. Their work was an example of using high cycles of concentration in cooling tower applications and preventing fouling with physical water treatment technology.

C. Fouling model development

In this section, a fouling model that predicts the fouling thermal resistance in heat exchangers is explained and it was verified with data from the present work and with data from the literature. The model, which was adapted from the Hasson-Quan model (Hasson, *et al.*, 1978; Quan *et al.*, 2008), considers the chemical dissociation and the mass transfer processes that occur when a water solution with mineral dissolved is heated and the temperature increases beyond the critical temperature of the solubility limits. The present model was specifically developed for refrigerant condensers used in chiller applications.

In agreement with Kern & Seaton (1959) work, the governing equation of fouling process is given in Eq. (7), where R_f is the fouling resistance, in m^2-K/W, m_d and m_r are the mass of fouling deposited and removed on the heat transfer surface, respectively, in g/m^2-s; and ρ_f and λ_f are the density and thermal conductivity of fouling deposit.

$$\frac{dRf}{dt} = \frac{m_d - m_r}{\rho_f \lambda_f} \tag{7}$$

Hasson *et al*. (1978) conducted a chemical reaction analysis in acid and alkaline solution to predict the mass of fouling deposit. Since medium and high fouling potential water have pH that ranged from 8.4 to 9.6, the fouling deposit rate in alkaline solutions from (Hasson, *et al.*, 1978) was applied in the present work and it yielded to Eq.(8). k_{sp} is the solubility product of calcium carbonate and it has a magnitude of 10^{-9} mol^2/L^2. The precipitation rate coefficient, k_R is temperature dependent and specific to fouling minerals. From authors previous work (Wu & Cremaschi, 2012), a chemical composition analysis was conducted on the water and on the fouling deposit. Samples of fouling deposits were taken from the inner surfaces of the TTHE heat exchanger at the end of the experiment and their chemical analysis indicated that more than 85% of the fouling deposit was calcium carbonate while the amount of magnesium, iron, copper, zinc and other elements were less than 5%. Therefore in the present model, calcium carbonate was assumed to be the only chemical species present in the fouling deposit. In Eq. (8), k_R is the precipitation rate coefficient, and it was calculated from Eq.(9), where R_g is universal gas constant, (1.986cal/K-mol) and T is water bulk temperature, in K.

$$m_d = k_D[CO_3^{2-}] \frac{1 - \frac{k_{sp}}{[Ca^{2+}][CO_3^{2-}]}}{1 + \frac{k_D}{k_R[CO_3^{2-}]} + \frac{[CO_3^{2-}]}{[Ca^{2+}]}} \tag{8}$$

$$lnk_R = 38.74 - \frac{20700}{R_g T} \tag{9}$$

k_D in Eq.(8) is the convective diffusion coefficient of calcium carbonate, which was estimated by using Eq. (10) from (Quan, *et al.*, 2008), where v is the flow velocity inside the heat exchanger and Re and Sc are Reynolds number and Schmidt number.

$$k_D = 0.023 \cdot v \cdot Re^{-0.17} \cdot Sc^{-0.67} \quad (10)$$

In agreement with Quan's model (Quan, *et al.*, 2008), the removal rate of fouling can be expressed by a proportionality law shown in Eq. (11), where δ_f is the thickness of fouling deposit.

$$m_r = c_r \rho_f \delta_f^{1.5} \quad (11)$$

The thickness of fouling is unknown in each test but $\rho_f \delta_f^{1.5}$ describes the instantaneous mass of fouling deposit. In the Hasson-Quan model, Eq. (11) was later modified and replaced with Eq. (12), where the removal coefficient c_r is shown in Eq.(13) and ψ is the deposition strength factor.

$$m_r = c_r m_d \quad (12)$$

$$c_r = \frac{0.00212 v^2}{{\lambda_f}^{0.5} \psi} \quad (13)$$

Based on the analysis above, by integrating Eq. (7) in time, the fouling thermal resistance was predicted. Comparison between the predicted fouling resistance and the experimental data from the present work are shown in Fig. 4 and Fig. 5, in which the fouling test data were conducted on a smooth TTHE and BPHE with corrugation angle 60° in high fouling potential water, respectively.

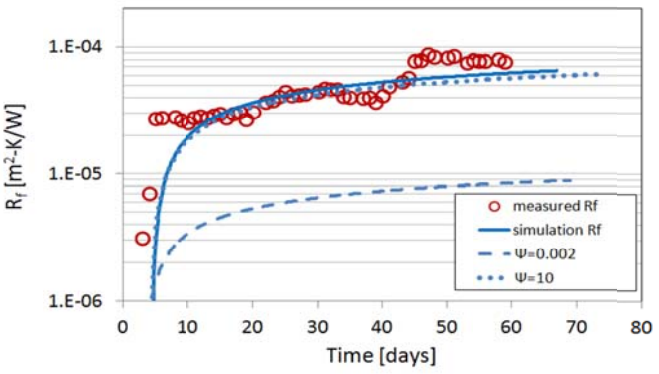

Fig. 4 Comparison of fouling model results with experimental data in a smooth tube-in-tube heat exchanger

Fig. 4 shows the comparison between experimental data and simulation results in a smooth tube-in-tube heat exchanger. The deposition strength factor is not known and a sensitivity study was conducted by considering that in the experiments the fouling thermal resistance increased asymptotically. Thus, the overall amount of fouling deposited increased but the removal process slowed its rate of increase with time. This means that in Eq. (13), the removal coefficient c_r must be in the range of $0 < cr < 1$. In addition, the fouling thermal resistance must always be greater than zero. These constraints provided a range of investigation for the deposition strength factor. ψ had a minimum value of 0.002 and while the maximum value has not theoretical constraints, by assessing the root mean square (RMS) error it was found that $\boldsymbol{\psi} = 1$ provided better accuracy of the model, as shown in Table 3. To improve the accuracy further the authors proposed that the deposition strength factor changed with the deposition thickness because this parameter describes the level of aggregation of the precipitate on the heat transfer surface. In this work the correlation (14) was proposed and the corresponding predicted thermal fouling resistance is shown as solid line in Fig. 4. Then, the same correlation was applied also for all the other cases, that is, for predicting the thermal fouling resistance in BHPEs and for the data from literature.

$$\begin{aligned} \psi(t) &= 1 && t = 1 \\ \psi(t) &= 0.99\, \psi(t-1) && t > 1 \end{aligned} \quad (14)$$

In Fig. 4, it is evident that during the first two weeks, the simulation results under predicted the fouling resistance while the simulations and the data are in good agreement thereafter. It should be noted that, our experiment was designed to initially circulate low fouling potential water in the cooling water loop and progressively concentrate the water to high fouling potential water in about two weeks. We monitored the water chemistry once a week, and $[Ca^{2+}]$ and $[\boldsymbol{CO_3^{2-}}]$ data between one week and the next one were assumed to vary linearly. Since water chemistry changed rapidly in the first two weeks and then remained fairly constant once it reached high fouling potential LSI, it is possible that the assumption of linear variation of the mineral concentration during the first two week is not representative. Another observation is that, the present model only considers fouling formation due to precipitation and it did not take into account the particulate fouling. However, as discussed in Fig. 3, in the first week of fouling test on TTHE, the water side pressure drop across the TTHE increased suddenly, which might have been a sign of localized flow blockage due to particulate fouling. Since the present model did not include particulate fouling, the fact that the simulation results under-predict the fouling resistance data can be expected.

Table 3 Sensitivity analysis of R_f with respect to ψ

ψ	RMS error $\times 10^5$
0.02	1.5329
1	1.3787
10	1.3795
Correlation in Eq. (14)	1.3782

Fig. 5 shows the comparison of the simulation results with the data for the fouling tests on BPHE with hard corrugation angle of 60° in high fouling potential water. With respect to the BPHEs with soft corrugation angle of 30°, the tested BPHE with hard corrugation angle had lower propensity to fouling and was less sensitive to mineral particles clogging the channels. The current model over predict slightly the fouling thermal resistance in the first two weeks. This might be due to the estimation of $[Ca^{2+}]$ and $[\ CO_3^{2-}\ ]$ during the concentration phase of the circulating water or it might be due to over estimation of ψ in the initial stage of fouling formation in the model. It is also possible that, the fouling deposition strength factor

depends on surfaces energy, particles type and shape, and local flow velocity and shear rates near the wall; all these variables were not included in the present model for ψ.

Further comparison of the present model was made by considering the fouling test data from the open literature. Fig. 6 shows the comparison of simulation results and experimental data of Karabelas *et al.*, (1997), in which a BPHE with corrugation angle of 30° was tested in high fouling potential water. Due to the high concentration of Ca^{2+}, the fouling tests only lasted for 220 hours before asymptotic fouling resistance was reached. In Fig. 6, the model predicted the asymptotic fouling resistance at different flow velocity and followed similar trends as indicated by the experimental data. Due to limited water chemistry information in the experimental data of Karabelas *et al.*, work, some assumptions on the water chemistry were made and the model underestimated the fouling resistance at the beginning of the fouling tests.

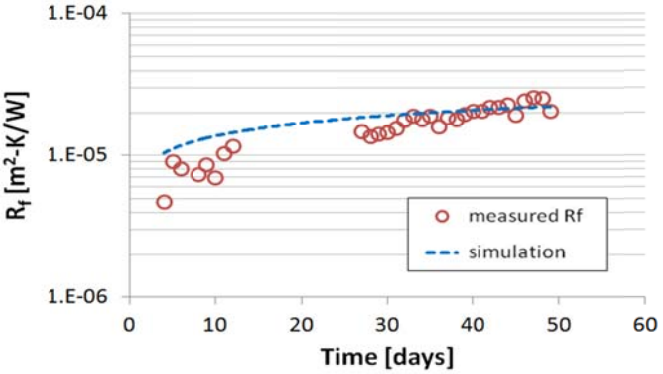

Fig. 5 Comparison of fouling model results with experimental data in BPHE (φ=60°)

In addition, experimental data on smooth tube in medium fouling potential water from (Webb & Li, 2000) was also applied to compare the modified Hasson-Quan model, and similar fouling trends were observed. However, since the water chemistry information was limited, the model over predicted the fouling resistance after three weeks of operation.

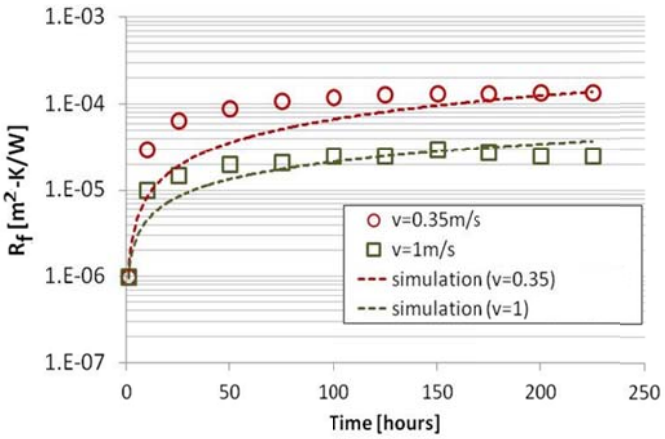

Fig. 6 Comparison of fouling model results with Karabelas data in BPHE (φ=30°)

The experimental work from (Quan, *et al.*, 2008) was finally included in the present comparison of the predicted thermal fouling resistance by the developed model with data from the literature. The tested fluid in Quan *et al.* had lower pH values and the fouling deposition model based on alkaline solution in the present model tended to under estimate the fouling resistance by 30% to 50%. The overall comparison between the simulation results of the present model and the experiment data from the present work and from the literature is summarized in Fig. 7. The present model predicted the fouling thermal resistance within 30% error in average. It generally under-predicted the fouling thermal resistance at the beginning stage of fouling formation and in the case of severe particulate fouling. More detailed information on type of mineral precipitation and local flow velocity near the wall of the heat exchangers might help to improve the accuracy of the present model and further research is needed to estimate the fouling deposition strength factor for various geometries.

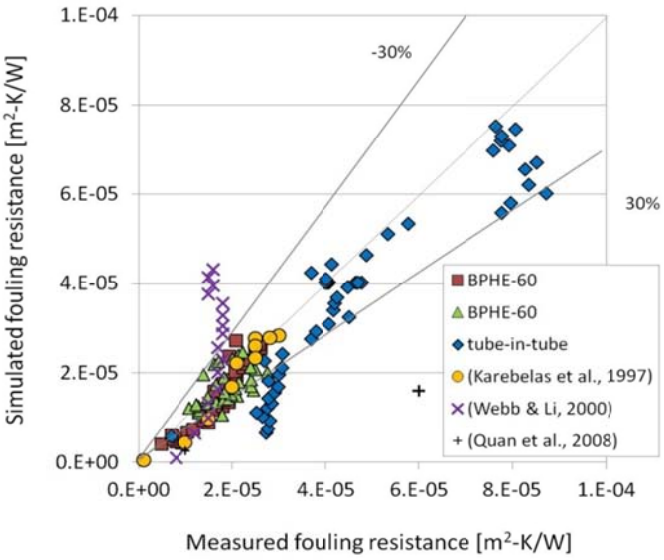

Fig. 7 Comparison between all test data and predicted fouling thermal resistance with present model

CONCLUSIONS

This paper presents the effect of fouling on the heat transfer performance of two brazed plate heat exchangers (BPHEs) and one smooth tube-in-tube heat exchanger (TTHE) with similar nominal heat transfer area. The amount of mineral precipitation on the heat transfer surfaces led to an additional thermal barrier. The fouling thermal resistance increased asymptotically and for TTHE it reached up to 42% of the convective thermal resistance of the water side in clean conditions. For BPHE with hard corrugation angle of 63° it reached up to 70% while for BPHE with corrugation angle of 30°, the additional thermal resistance due to fouling was 3.19 times. This extreme case might have been due to localized flow blockage due to partially blocked channels in the BPHE by particulate fouling, which was observed experimentally in the data for this BPHE.

The fouling formation inside heat exchangers penalizes both thermal and hydraulic performance. A model for the species dissociation and mineral precipitation on the heat transfer surfaces was developed based on the existing approaches in the literature. The present model was

compared with experimental data from the present work as well as fouling test data in the literature. Information on the type of mineral precipitation and local flow velocity near the internal walls of the heat exchanger are keys to obtain an accurate prediction on fouling deposition strength factor. Very limited work exists in the literature and this parameter was estimated from the data of TTHE in the present work. By considering the same fouling deposition strength factor for all other cases, the simulation results predicted the fouling thermal resistance with an average error of 30%.

NOMENCLATURE

BPHE	brazed plate heat exchanger	
$[Ca^{2+}]$	calcium concentration	ppm
$[Cl^-]$	chloride concentration	ppm
$[CO_3^{2-}]$	carbonate concentration	ppm
c_r	removal coefficient	dimensionless
cycle	concentration cycle	dimensionless
k_D	convectivediffusion coefficient	dimensionless
k_R	precipitation rate coefficient	dimensionless
k_{SP}	solubility product	mol^2/L^2
LSI	Langelier Saturation Index	dimensionless
m	mass	g/m^2-s
$M_{alklinity}$	"M" alkalinity	ppm
ΔP	pressure drop	kPa
PDPF	pressure drop penalty factor	dimensionless
R	thermal resistance	m^2-K/W
Re	Reynolds number	dimensionless
Rg	universal gas constant	cal/K-mol
t	time	hours or days
T	temperature	°C or K
TDS	total dissolved solid	ppm
TTHE	tube-in-tube heat exchanger	
v	velocity	m/s
φ	corrugation angle	degree
ρ	density	kg/m^3
δ	fouling thickness	m
ψ	deposition strength factor	dimensionless
λ	thermal conductivity	W/m-K

Subscript

c	clean	makeup	makeup water
circulate	Circulate water	r	removal
d	deposit	ref	refrigerant
f	fouled or fouling	sat	saturated solution
ff	fluid film	tot	total
k	conduction	w	water

REFERENCES

Ayub, Z. H., 2003. Plate heat exchanger literature survey and new heat transfer and pressure drop correlations for refrigerant evaporators. *Heat Transfer Engineering, v*(24), 3-16.

Betz. 1991. Handbook of industrial water conditioning, 9th ed. Trevose, PA, USA.

Beychok, M. R., 1952. How to calculate cooling tower control variables. *Petroleum Processing, v*(7), 1452-1456.

Chamra, L. M., & Webb, R. L., 1994. Modeling liquid-side particulate fouling in enhanced tubes. *International Journal of Heat and Mass Transfer, v*(37), 571-579.

Cho, Y. I., Kim, W. T., & Cho, D., 2006. Fouling mitigation in a heat exchanger: High cycles of concentration for a cooling-tower application. *Experimental Heat Transfer, 19*(2), 113-128.

Cho, Y. I., Lee, S., & Kim, W., 2003. *Physical water treatment for the mitigation of mineral fouling in cooling-tower water applications.* In: Proceedings of 2003 ASHRAE Winter Meeting Technical paper, January 26, 2003 - January 29, 2003, Chicago, IL, United states.

Cremaschi, L., Barve, A., & Wu, X., 2012. Effect of condensation temperature and water quality on fouling of brazed-plate heat exchangers. *ASHRAE Transactions, 118*(PART 1), 1086-1100.

Cremaschi, L., Spitler, J. D., Lim, E., & Ramesh, A., 2011. Waterside fouling performance in brazed-plate-type condensers for cooling tower applications. *HVAC & R Research, 17*(2), 198-217.

Flynn, D. J., & Nalco, C. (2009). The Nalco water handbook. from http://www.knovel.com/knovel2/Toc.jsp?BookID=2799

Grandgeorge, S., Jallut, C., & Thonon, B., 1998. Particulate fouling of corrugated plate heat exchangers. Global kinetic and equilibrium studies. *Chemical Engineering Science, 53*(17), 3050-3071.

Haider, S. I., Webb, R. L., & Meitz, A. K., 1991. *Survey of water quality and its effect on fouling in flooded water chiller evaporators.* In: Proceedings of ASHRAE Winter Meeting - Technical Papers, January 19, 1991 - January 23, 1991, New York, NY, USA.

Hasson, D., Sherman, H., & Biton, M., 1978. Prediction of Calcium Carbonate Scaling Rates. *v*(2), 193-199.

Incropera, F. P., D.P., D., Bergman, T. B., & Lavine, A. S., 2006. *Fundamental of heat and mass transfer.* (6th ed.). New York, NJ, USA: John Wiley & Sons.

Karabelas, A. J., Yiantsios, S. G., Thonon, B., & Grillot, J. M., 1997. Liquid-side fouling of heat exchangers. An integrated R D approach for conventional and novel designs. *Applied Thermal Engineering, v*(17), 727-737.

Kern, D. Q., & Seaton, R. E., 1959. A theoretical analysis of thermal surface fouling. *British Chemical Engineering, 4*(5), 258-262.

Langelier, W. F., 1936. The analytical control of anti-corrosion water treatment. *Journal of American Water Works Association, 28*(10), 1500-1521.

Quan, Z. H., Chen, Y. C., & Ma, C. F., 2008. Heat mass transfer model of fouling process of calcium carbonate on heat transfer surface. *Science in China Series E-Technological Sciences, 51*(7), 882-889.

Thonon, B., Grandgeorge, S., & Jallut, C., 1999. Effect of geometry and flow conditions on particulate fouling in plate heat exchangers. *Heat Transfer Engineering, v*(20), 12-24.

Walker, R., 1976. Corrosion Inhabition of Copper by Tolylriazole. *Corrosion, v*(32), 339-341.

Webb, R. L., & Li, W., 2000. Fouling in enhanced tubes using cooling tower water Part I: Long-term fouling data. *International Journal of Heat and Mass Transfer, v*(43), 3567-3578.

Wu, X., & Cremaschi, L., 2012. *Thermal and chemical analysis of fouling phenomenon in condensers for cooling tower applications.* In: Proceedings of 14th International Refrigeration and Air Conditioning conference at Purdue, Paper No.2198, July 16, 2012 - July 19, 2012, West Lafayette, Indiana, United States